1 **Dynamics of brain function in chronic pain patients assessed**

2 **by microstate analysis of resting-state electroencephalography**

3
4
5 Elisabeth S. May[1,2*], Cristina Gil Ávila[1,2*], Son Ta Dinh[1,2], Henrik Heitmann[1,2,3], Vanessa D.

6 Hohn[1,2], Moritz M. Nickel[1,2], Laura Tiemann[1,2], Thomas R. Tölle[1,3], Markus Ploner[1,2,3]

7 [*] Both authors contributed to this work equally.

8

9 [1]Department of Neurology, School of Medicine, Technical University of Munich (TUM), Munich,

10 Germany; [2]TUM-Neuroimaging Center, School of Medicine, TUM, Munich, Germany; [3]Center

11 for Interdisciplinary Pain Medicine, School of Medicine, TUM, Munich, Germany

12
13
14
15
16
17
18
19

20

21

22

23

24 **Correspondence to:**

25 Markus Ploner, Department of Neurology, Technical University of Munich (TUM), Ismaninger

26 Str. 22, 81675 Munich, Germany, Phone +49-89-4140-4608, markus.ploner@tum.de

27

28

29 37 text pages, 4 figures, 7 tables

Abstract

Chronic pain is a highly prevalent and severely disabling disease, which is associated with substantial changes of brain function. Such changes have mostly been observed when analyzing static measures of brain activity during the resting-state. However, brain activity varies over time and it is increasingly recognized that the temporal dynamics of brain activity provide behaviorally relevant information in different neuropsychiatric disorders. Here, we therefore investigated whether the temporal dynamics of brain function are altered in chronic pain. To this end, we applied microstate analysis to eyes-open and eyes-closed resting-state electroencephalography (EEG) data of 101 patients suffering from chronic pain and 88 age- and gender-matched healthy controls. Microstate analysis describes EEG activity as a sequence of a limited number of topographies termed microstates, which remain stable for tens of milliseconds. Our results revealed that sequences of 5 microstates, labelled with the letters A to E, described resting-state brain activity in both groups and conditions. Bayesian analysis of the temporal characteristics of microstates revealed that microstate D has a less predominant role in patients than in healthy participants. This difference was consistently found in eyes-open and eyes-closed EEG recordings. No evidence for differences in other microstates was found. As microstate D has been previously related to attentional networks and functions, abnormalities of microstate D might relate to dysfunctional attentional processes in chronic pain. These findings add to the understanding of the pathophysiology of chronic pain and might eventually contribute to the development of an EEG-based biomarker of chronic pain.

Key words: chronic pain, dynamics, EEG, microstate analysis, resting-state

1 ## 1. Introduction

2 Chronic pain is a highly disabling disease, which affects 20-30% of the adult population [7; 24].

3 Its pathophysiology is not fully understood and treatment is often insufficient [59], imposing a

4 tremendous burden on patients, health care systems and society [46]. Converging lines of

5 evidence have shown that chronic pain is associated with extensive changes of brain structure

6 and function [2; 29]. Understanding these changes promises fundamental insights into the

7 underlying pathophysiology and might eventually help to establish a much sought-after

8 biomarker of chronic pain [14; 57].

9 Brain function in chronic pain has mostly been assessed using functional magnetic

10 resonance imaging (fMRI) [2] and electro-/magnetoencephalography (EEG/MEG) [44]. Most

11 of these studies have analyzed static measures of brain activity during the resting-state,

12 usually by aggregating a certain feature of brain function across several minutes. However,

13 brain activity varies over time and it is increasingly recognized that these temporal dynamics

14 provide behaviorally and clinically relevant information, which complements static measures

15 [19; 45]. Correspondingly, it has been proposed that the dynamics of brain activity and

16 connectivity critically shape the perception of pain [28]. By assessing brain activity and

17 connectivity at ultra-low frequencies below 0.1 Hz, recent fMRI studies have provided support

18 for this concept in chronic pain (e.g. [3; 5; 10; 58]). However, the temporal dynamics of chronic

19 pain-related brain activity at frequencies higher than 1 Hz have not been consistently explored

20 yet.

21 EEG and MEG are well suited to study such dynamic changes of brain activity at higher

22 frequencies. One of the best-established methods in this field is microstate analysis (see [25;

23 34] for reviews), which has revealed that temporal changes of EEG activity do not occur

24 randomly. Instead, EEG activity switches between a limited number of so-called microstates.

25 During a microstate, the EEG topography remains stable for tens of milliseconds before

26 abruptly transitioning to another microstate. EEG resting-state activity is usually well-described

27 with 4 to 6 microstates, which are remarkably similar across participants. Thus, microstate

28 analysis quantifies resting-state EEG recordings as sequences of a limited number of

1   microstates. The temporal characteristics of these microstates carry important information

2   about mental processes [6; 34]. Moreover, abnormalities of temporal microstate characteristics

3   have been observed in different neuropsychiatric disorders (e.g. [12; 38; 48]). During the

4   writing of this manuscript, a first microstate study in patients suffering from chronic pain was

5   published. The results showed lower occurrence and time coverage of microstate C in patients

6   with fibromyalgia [20]. However, these findings need to be replicated and extended to other

7   chronic pain conditions.

8   Here, we investigated whether the temporal dynamics of brain activity are changed in

9   a large cohort of patients suffering from chronic pain. To this end, we applied microstate

10 analysis to EEG resting-state recordings of 101 patients suffering from different types of

11 chronic pain and 88 matched healthy control participants. Thereby, the study aimed to further

12 the understanding of the pathophysiology of chronic pain and to potentially contribute to the

13 development of a brain-based biomarker of chronic pain.

2. Materials and methods

2.1. Participants

The current study represents a re-analysis of previously published data obtained at the Technical University of Munich for the large-scale study of brain dysfunction in chronic pain [54]. 101 patients (69 women; age = 58.1 ± 13.6 years [mean ± SD]) suffering from different types of chronic pain and 88 age- and sex-matched healthy controls (60 women, age = 57.5 ± 14.2 years) participated in the study. Inclusion criteria for patients were a clinical diagnosis of chronic pain, with pain lasting at least 6 months, and a minimum reported average pain intensity of at least 4 out of 10 during the past 4 weeks (0 = no pain, 10 = worst imaginable pain). Exclusion criteria for patients were acute changes of the pain condition during the past 3 months (e.g. due to recent injuries or surgeries), major neurological diseases (e.g. epilepsy, stroke or dementia), major psychiatric diseases aside from depression and severe general diseases. Patients taking benzodiazepines were also excluded. Other medication was not restricted and was maintained. In total, 47 patients with chronic back pain, 30 patients with chronic widespread pain, 6 patients with joint pain and 18 patients with neuropathic pain were included in the study. Exclusion criteria for healthy participants were a past medical history of pain lasting more than 6 months, having any pain on the day of testing, surgery or acute injury during the last 3 months and any neurological or psychiatric diseases. All participants provided written informed consent. The study was approved by the ethics committee of the Medical Faculty of the Technical University of Munich and conducted according to the relevant guidelines and regulations.

Questionnaires were used to assess pain characteristics and comorbidities on the day of the recording. All patients completed the following questionnaires: pain characteristics were assessed by the short-form McGill pain Questionnaire (SF-MPQ) [33], depression by the Beck Depression Inventory II (BDI-II) [4] and anxiety by the State-Trait Anxiety Inventory (STAI) [52]. The medication was quantified for all patients using the Medication Quantification Scale (MQS) [21]. 81 patients additionally completed the painDETECT questionnaire [18] to assess the neuropathic pain component and 47 patients completed the Pain Disability Index (PDI) [16]

1   and the Veteran's RAND 12-Item Health Survey (VR-12) [50] to assess pain disability and

2   quality of life, respectively. All healthy control participants completed BDI-II and STAI

3   questionnaires to assess potential comorbidities. Detailed characteristics of the participants

4   can be found in Table 1.

5

6   **2.2. Recordings**

7   Brain activity was recorded using electroencephalography (EEG) during the resting-state.

8   Participants were instructed to stay in a wakeful and relaxed state without performing any

9   particular task. Two 5-min blocks of continuous resting-state data were recorded, one with

10   eyes closed and the other with eyes open. The temporal order of the blocks was counter-

11   balanced. During the recording, participants were comfortably seated and listened to white

12   noise played through headphones to mask any ambient noise.

13   Data were recorded with 64 electrodes and a BrainAmp MR plus amplifier (Brain

14   Products, Munich, Germany). The electrodes included all electrodes from the 10-20

15   international system and the additional electrodes Fpz, CPz, POz, Oz, Iz, AF3/4, F5/6,

16   FC1/2/3/4/5/6, FT7/8/9/10, C1/2/5/6, CP1/2/3/4/5/6, TP7/8/9/10, P1/2/5/6/7/8 and

17   PO3/4/7/8/9/10 (Easycap, Herrsching, Germany). Two electrodes were placed below the outer

18   canthus of each eye to monitor eye movements. All EEG electrodes were referenced to FCz

19   and grounded at AFz. For 81 patients and 69 healthy controls, muscle activity was

20   simultaneously recorded with two bipolar electromyography (EMG) electrode montages and a

21   BrainAmp ExG MR amplifier (Brain Products, Munich, Germany). EMG electrodes were placed

22   on the right masseter and neck (semispinalis capitis and splenius capitis) muscles [13]. The

23   EMG ground electrode was placed at vertebra C2. Data were obtained at a sampling frequency

24   of 1000 Hz, with 0.1 μV resolution and were band-pass filtered online between 0.016 and 250

25   Hz. Impedances were kept below 20 kΩ.

26

2.3. Preprocessing

Preprocessing was performed with the Brain Vision Analyzer software (Brain Products, Munich, Germany) on the appended data from the eyes-open and the eyes-closed conditions. For artifact identification, a high pass filter at 1 Hz and a notch filter at 50 Hz were applied to remove low frequency drifts and electrical line noise, respectively. Independent Component Analysis was performed [23]. Components representing eye movements and muscle artifacts were identified based on their time courses and topographies and subtracted from the raw unfiltered EEG time series [60]. Signal jumps higher than ± 100 µV and their adjacent time intervals (200 ms before and after the jump) were marked for rejection. Subsequently, all data sets were visually inspected and remaining bad intervals were marked for rejection. Finally, data were re-referenced to the average reference and the reference electrode FCz was added to the electrode array.

2.4. Microstate analysis

Microstate analysis was performed using the free academic software Cartool version 3.8 (Brunet et al., 2011), Matlab (Mathworks, Natick, MA) and the Matlab toolbox Fieldtrip [41]. Analyses were performed separately for the eyes-open and eyes-closed conditions. For all analyses, the first minute of artifact-free continuous data of each condition was selected. Subsequently, the selected data segment was band-pass filtered between 1 and 40 Hz and down-sampled to 125 Hz, in line with previous studies (Britz, Van De Ville and Michel, 2010; Custo et al., 2017; Tomescu et al., 2018). Eyes-closed data of 1 chronic pain patient and 1 healthy control and eyes-open data of 11 patients and 8 controls had to be excluded from further analysis because no continuous one-minute artifact-free segment was available. Thus, final sample sizes were 100 patients and 87 healthy controls for the eyes-closed condition and 90 patients and 80 healthy controls for the eyes-open condition. An overview of the microstate analysis pipeline can be found in Figure 1.
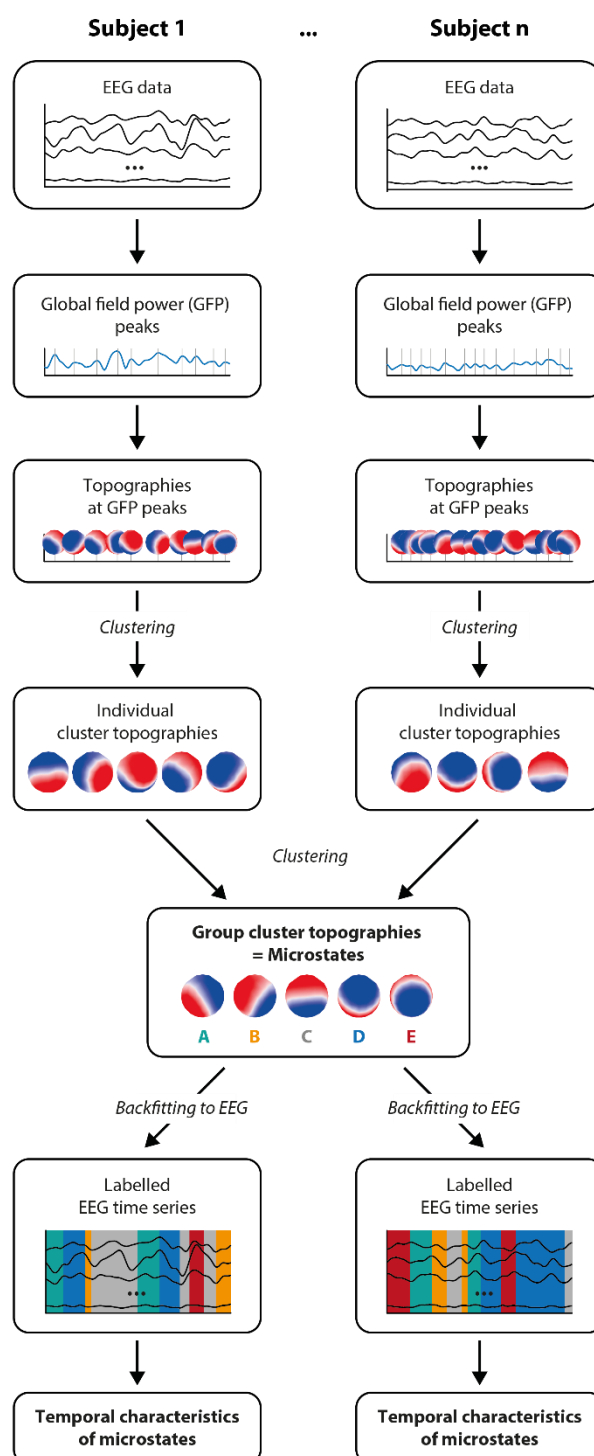
Figure 1. Microstate analysis. For each participant, the global field power (GFP) is calculated and topographies at GFP peaks are selected for individual clustering. Topographies at GFP peaks are clustered with a modified k-means clustering, leading to a variable number of individual cluster topographies per individual. Next, individual cluster topographies are concatenated and clustered on a group level. This resulted in 5 different group cluster topographies, labelled as microstates A to E. Microstate topographies are then fitted back to the individual EEG data, resulting in a labelled EEG time series in which each time point is associated to a microstate. From the labelled EEG time series, the temporal characteristics of microstates are derived. This analysis was performed separately per group (chronic pain patients and healthy participants) and condition (eyes-open and eyes-closed).

1   *2.4.1. Definition of microstates*

2   We defined microstates through a well-established two-step clustering procedure using a

3   modified k-means algorithm [42]. In line with previous studies [12; 38; 48; 55], this was done

4   separately for each group and condition.

5   The first step consisted of a k-means clustering performed at the individual level. For

6   each participant, EEG topographies at global field power (GFP) peaks were clustered, yielding

7   a variable number of individual-level topographies. The GFP is a measure of the instantaneous

8   strength of EEG activity measured over the whole scalp and mathematically defined as the

9   standard deviation of the signals of all electrodes [39]. EEG topographies were clustered at

10   GFP maxima since they represent the time points of highest signal-to-noise ratio [39; 42].

11   The clustering algorithm requires an a priori definition of k, which is the number of

12   clusters into which the data will be grouped. To select the optimal number of clusters, we

13   performed the clustering with different numbers of k = 4 to 12 initial clusters, following Cartool's

14   default settings for resting-state data. First, an initial number of k topographies was randomly

15   selected from all GFP-peak topographies of the individual EEG time series. Second, the

16   selected topographies were spatially correlated with the remaining topographies at GFP peaks,

17   ignoring polarity. Third, the topographies at GFP peaks were assigned to the cluster with the

18   highest spatial correlation. If the highest correlation was smaller than 0.5, the topography was

19   not assigned to any cluster. Fourth, the center of each cluster was computed, resulting in k

20   new "average" cluster topographies. The new cluster topographies were then again correlated

21   with the topographies at GFP peaks, closing the loop. The algorithm stopped when the

22   variance of the clusters converged to a limit. In order to overcome the random selection of the

23   initial cluster topographies, the clustering was repeated 100 times per set of k clusters and the

24   set explaining most variance of the data was selected. The optimal number of clusters was

25   identified for each individual separately according to a meta-criterion with 7 independent

26   optimization criteria (for more details refer to [6]). This procedure resulted in 4 to 8 topographies

27   for each participant and condition. The number of individual topographies did not differ

28   between groups for the eyes-open or the eyes-closed condition (eyes-closed: mean$_{patients}$ =

1 5.020, mean$_{controls}$ = 4.919, t = -0.727, p = 0.468, BF$_{10}$ = 0.204, median δ = -0.099, 95% CI = [-

2 0.377, 0.178]; eyes-open: mean$_{patients}$ = 4.944, mean$_{controls}$ = 4.912, t = -0.256, p = 0.799, BF$_{10}$

3 = 0.171, median δ = -0.036, 95% CI = [-0.326, 0.253]; two-sided independent samples t-tests).

4 In the second step, a second k-means clustering was performed at group level,

5 clustering the concatenated individual topographies obtained in the previous step. Cartool's

6 default settings for the second clustering were adopted, i.e. an initial number of k = 4 to 15

7 clusters and 200 k-means initializations. Again, the polarity was ignored and a maximum

8 correlation higher than 0.5 was needed for cluster assignment. The same meta-criterion as

9 before was used to identify the optimal number of clusters on a group level. It consistently

10 revealed an optimal number of 5 group-level topographies for each group and condition.

11 Each set of 5 group-level topographies (Figure 2) was visually inspected and compared

12 to topographies reported in the literature. For both groups, the first four topographies closely

13 resembled the four well-known 'canonical' microstates A to D reported previously and were

14 labeled accordingly [25; 27; 34]. The topography of the fifth microstate closely resembled a

15 microstate, which has been consistently reported in more recent studies [6; 11; 62], since an

16 increasing number of studies is now using a data-driven approach to define the optimal number

17 of microstates. We labeled it with the letter E. Throughout the manuscript, the 5 group-level

18 topographies are referred to as microstates A to E. Similarities and differences of microstate

19 topographies between groups were assessed by calculating spatial correlations and

20 topographic analyses of variance (TANOVA) for all microstates (A to E), respectively. The

21 spatial correlation is a scalar value computed as the Pearson's correlation coefficient between

22 all matched electrodes of two different topographies [39]. TANOVA is a non-parametric

23 randomization test based on the global map dissimilarity of individual topographies [39]. The

24 global map dissimilarity is a measure of the difference between two topographies directly

25 related to the spatial correlation [39]. For each microstate, global map dissimilarity was

26 computed between the microstate topographies of the patient and control groups using Cartool

27 [9]. To obtain a p-value, this dissimilarity was compared to a distribution of dissimilarities, which

28 was generated by randomly shuffling individual topographies between patient and control

1   groups and re-computing the dissimilarity between the center topographies of the randomized

2   groups. The process was repeated 5000 times. This comparison resulted in a p-value per

3   microstate, which was given by the proportion of permutations in which the dissimilarity was

4   smaller than the dissimilarity originally observed in the data. For both the eyes-closed and

5   eyes-open conditions, resulting p-values were corrected for multiple comparisons across the

6   5 microstate classes using the False Discovery Rate (FDR) [61].

7

8   *2.4.2. Temporal microstate characteristics*

9   Next, we determined the temporal characteristics of the five microstates for both groups. To

10   this end, individual EEG time series were construed as time series of microstates through a

11   'fitting procedure', i.e. a microstate was assigned to every time point. For each participant, the

12   EEG topographies of all time points were spatially correlated to the five microstate

13   topographies of the participant's group (patients/controls), ignoring polarity. Next, each EEG

14   time point was assigned to a microstate (A to E). To ensure a certain continuity in the

15   microstate time series, the relabeling was performed based on two criteria: (1) the correlation

16   should be high and (2) the majority of the surrounding time points should belong to the same

17   microstate [9]. To fulfill this compromise between goodness of fit and smoothness, standard

18   temporal smoothing (window half size = 5 and strength (Besag factor) = 10) was applied [42;

19   55]. No label was assigned if the highest spatial correlation was smaller than 0.5. On average,

20   the percentage of unlabeled time points was smaller than 0.2% and no differences existed

21   between groups in any condition (eyes-closed: $mean_{patients}$ = 0.077 %, $mean_{controls}$ = 0.072 %, t

22   = -0.308, p = 0.758, BF_{10} = 0.224, median δ = 0.166, 95% CI = [-0.319, 0.235]; eyes-open:

23   $mean_{patients}$ = 0.177 %, $mean_{controls}$ = 0.106 %, t = -0.875, p = 0.383, BF_{10} = 0.2237, median δ =

24   -0.124, 95% CI = [-0.416, 0.165]; two-sided independent samples t-tests).

25   Based on the time series of microstates, four measures were calculated to quantify the

26   temporal characteristics of each microstate: mean duration, time coverage, frequency of

27   occurrence and global explained variance (GEV). The mean duration is the average time (in

28   milliseconds) for which a microstate persists before transitioning to a different microstate. The

1 time coverage is the percentage of total time that a microstate is present. The frequency of

2 occurrence is the number of times that a microstate recurs per second. The global explained

3 variance is the percentage of global variance that is explained by every microstate.

4   Finally, we investigated the microstate sequence by examining the transition

5 probabilities from each microstate to the others [31; 40; 55]. To this end, we computed the

6 matrix of transition counts among all microstates for each participant and divided it by the

7 overall count of transitions.

8

9 **2.5. Statistical analysis**

10 Group differences of temporal microstate measures (mean duration, time coverage, frequency

11 of occurrence and global explained variance) and transition probabilities were analyzed in

12 JASP version 0.13.1 [22] using two-sided independent sample t-tests in both frequentist and

13 Bayesian frameworks. For the frequentist approach, significance level was set to 0.05. For p-

14 values of temporal measures, FDR correction was performed in Matlab (Mathworks, Natick,

15 MA) across the 5 microstates and the 4 different temporal measures, resulting in a correction

16 for 20 statistical tests per condition (eyes-open/eyes-closed). For the transition matrix, FDR

17 correction was performed across all 20 transitions per condition (eyes-open/eyes-closed). For

18 the Bayesian analysis, default priors (Cauchy distributions with a scale parameter r = 0.707)

19 were used. In addition to t-values and FDR-corrected p-values, results are reported using the

20 two-tailed Bayes factor BF_{10}. Effect size estimates for the BF_{10} are reported as the median of

21 the posterior Cohen's δ distribution together with its 95% credibility interval.

22   Finally, we investigated relationships between temporal microstate measures and

23 clinical parameters, using JASP version 0.13.1 [22]. To this end, temporal microstate

24 measures of microstate D (mean duration, time coverage, frequency of occurrence, global

25 explained variance) were selected for a correlation analysis, since they consistently showed

26 at least moderate evidence for a difference between patients and controls in both conditions

27 in the previous analysis. Pearson's correlations were calculated between the microstate

28 measures and major clinical parameters, which were available for all patients (current pain

1   intensity, SF-MPQ total pain score, depression (BDI) and medication (MQS)). Correlations

2   were again calculated in both frequentist and Bayesian frameworks. In the Bayesian analysis,

3   default priors (stretched beta priors with width = 1) were used. Results are reported using the

4   Pearson's correlation coefficient, its FDR-corrected p-value, its Bayes factor (BF_{10}) and the

5   95% credibility interval of the correlation coefficient. FDR correction of p-values was performed

6   in Matlab (Mathworks, Natick, MA) across all 16 performed correlations separately for each

7   condition (eyes-open/eyes-closed).

8

9   **2.6. Data and code availability**

10   Raw and preprocessed EEG data in BIDS format [43] as well as scripts for statistical analyses

11   are openly available at osf.io.

3. Results

2   The current study investigated whether the dynamics of resting-state brain activity are altered

3   in patients suffering from chronic pain. We performed microstate analysis, which describes the

4   time course of EEG activity as a sequence of a limited number of short stable topographies

5   termed microstates. We applied microstate analysis to eyes-open and eyes-closed resting-

6   state EEG activity and compared temporal characteristics of microstates between a large

7   cohort of patients suffering from chronic pain and age- and sex-matched healthy control

8   participants.

9

3.1. Definition of microstates A to E in patients and controls

11 We identified microstates using a standard two-step k-means clustering procedure [42]. The

12 procedure consistently revealed 5 different microstates in both groups and conditions (Fig. 2).

13 In accordance with previous studies [6; 8; 11; 26; 27; 34; 35; 62], the microstates were labeled

14 as microstates A to E. Together, the five microstate explained 79.63% and 80.15% of the

15 variance across individuals in the eyes-closed condition and 80.35% and 79.95% in the eyes-

16 open condition (chronic pain patients and healthy controls, respectively), which is in good

17 accordance with previous studies [12; 34; 49]. Figure 2 shows the topographies of both groups.

18 The high similarity of topographies between groups was confirmed by high spatial correlations

19 (eyes-closed: microstate A: r = 0.95, B: r = 0.93, C: r = 0.97, D: 0.89, E: r = 0.83; eyes-open:

20 microstate A: r = 0.98, B: r = 0.99, C: r = 0.99, D: r = 0.96, E: r = 0.99). In addition, TANOVAs

21 revealed subtle group differences between topographies hardly visible to the naked eye (eyes-

22 closed: microstate A: p = 0.014, B: p < 0.001, C: p < 0.001, D: p < 0.001, E: p < 0.001; eyes-

23 open: A: p = 0.005, B: p = 0.53, C: p < 0.001, D: p < 0.001, E: p = 0.31).

24   Taken together, the clustering procedures for both groups and conditions resulted in 5

25 microstate topographies, which were largely similar between groups.
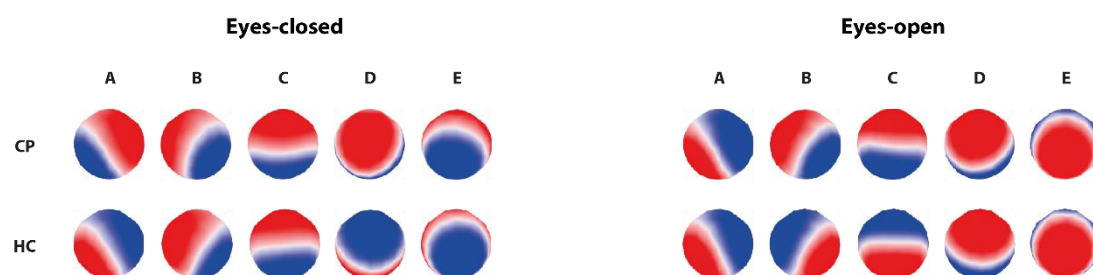
Figure 2. Microstate topographies of chronic pain patients and healthy participants for the eyes-closed and eyes-open conditions. Microstates were labelled with the letters A to E according to previous literature [34]. CP: Chronic pain; HC: Healthy control.

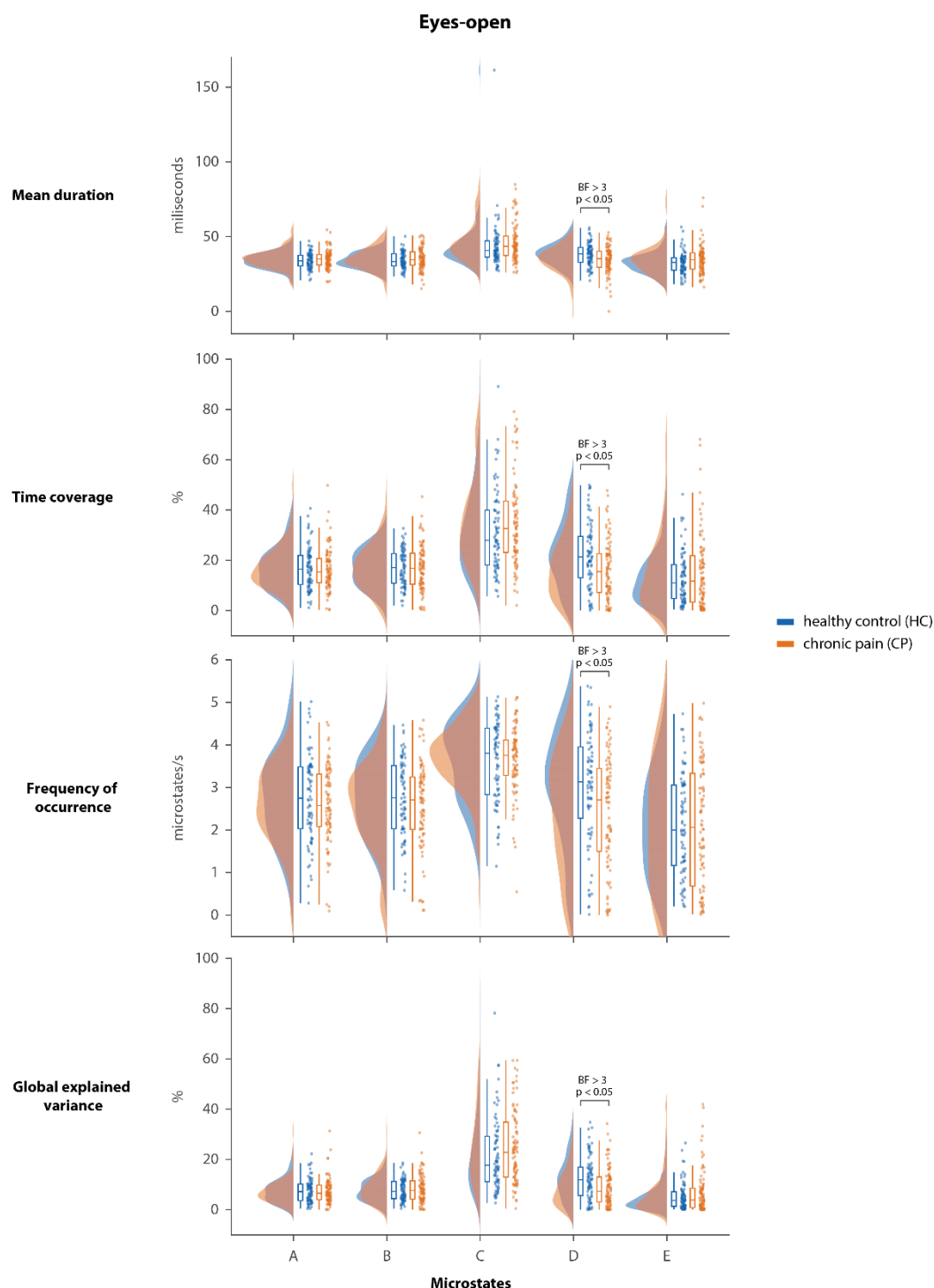## 3.2. Temporal characteristics of microstates in patients and controls

To investigate the dynamics of brain activity, we next analyzed whether the temporal characteristics of the 5 microstates differed between patients and healthy controls. To this end, microstates were back-fitted to the individual EEG time series by correlating microstate topographies with the EEG topographies at every time point. This allowed to assign each time point to a microstate, and, thus, to construe the EEG time series as time series of microstates.

We specifically calculated the mean duration, time coverage, frequency of occurrence and global explained variance of each microstate. This was done for each patient and each healthy control participant for the eyes-closed (Figure 3) and eyes-open (Figure 4) conditions. We next compared these temporal microstate characteristics between groups. The results revealed that all microstate D characteristics differed between patients and healthy participants. Such differences were consistently found in both conditions. In the eyes-closed condition, we found very strong evidence for a lower global explained variance of microstate D in patients compared to controls (Table 2; $BF_{10} > 300$, FDR-corrected p-value = 0.001). In addition, we found moderate evidence for a shorter mean duration, lower time coverage and lower frequency of occurrence of microstate D (Table 2; $3 < BF_{10} < 10$, FDR-corrected p-values < 0.05). Similarly, in the eyes-open condition, the data provided moderate evidence for a shorter mean duration, lower time coverage, lower frequency of occurrence and lower global explained variance of microstate D in chronic pain patients (Table 3; $3 < BF_{10} < 10$, FDR-corrected p-values < 0.05). For all other microstates, we did not find evidence for group differences consistent across measures and conditions (Tables 2 and 3).

15
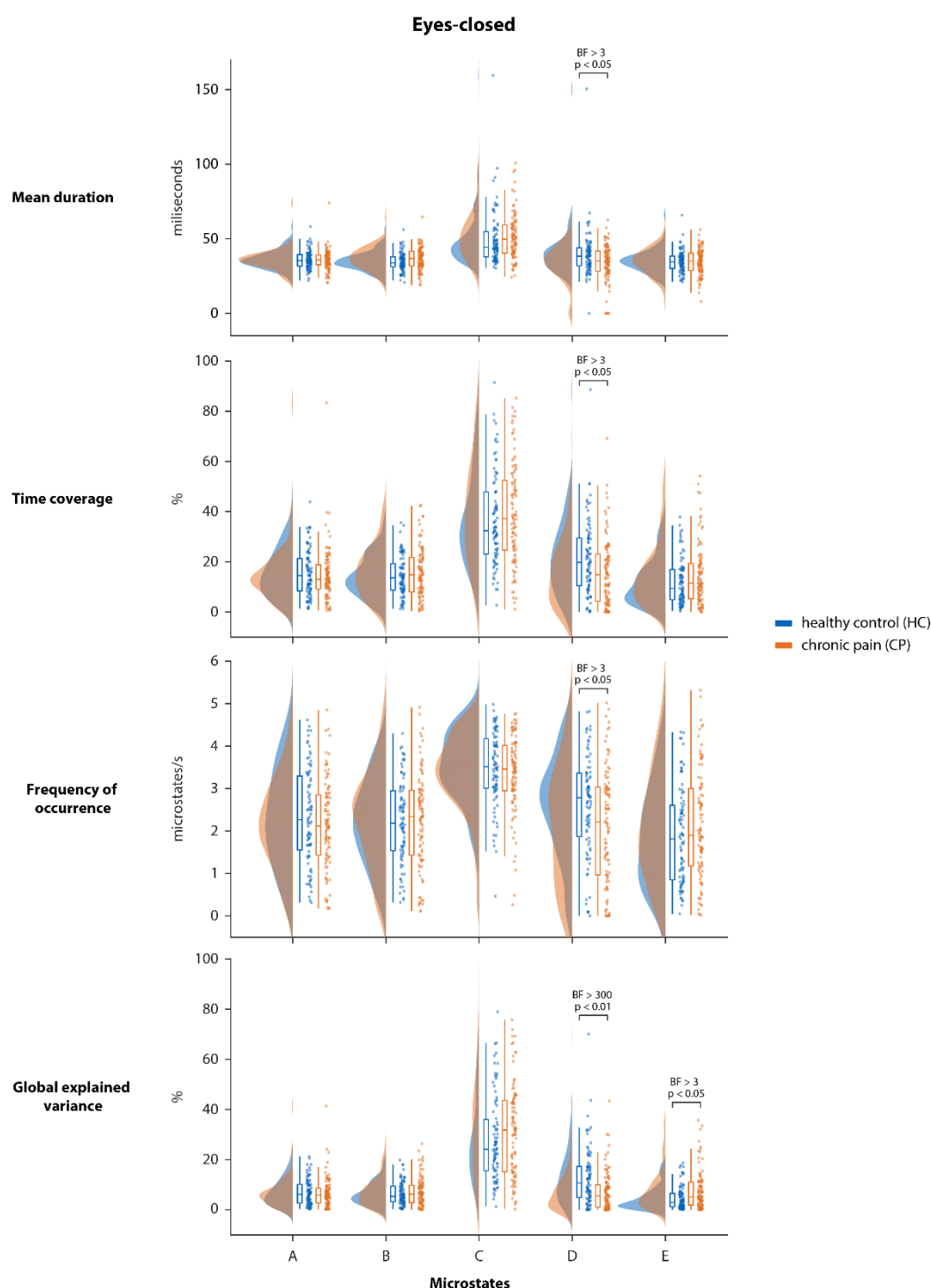
Figure 3. Temporal microstate characteristics in the eyes-closed condition. Mean duration, time coverage, frequency of occurrence and global explained variance of each microstate were calculated for both chronic pain patients and healthy controls. Raincloud plots [1] show un-mirrored violin plots displaying the probability density function of the data, boxplots, and individual data points. Boxplots depict the sample median as well as first (Q1) and third quartiles (Q3). Whiskers extend from Q1 to the smallest value within Q1 − 1.5* interquartile range (IQR) and from Q3 to the largest values within Q3 + 1.5* IQR. BF = Bayes Factor in favor of the alternative hypothesis.

16

Figure 4. Temporal microstate characteristics in the eyes-open condition. Mean duration, time coverage, frequency of occurrence and global explained variance of each microstate were calculated for chronic pain patients and healthy controls. Raincloud plots [1] show un-mirrored violin plots displaying the probability density function of the data, boxplots, and individual data points. Boxplots depict the sample median as well as first (Q1) and third quartiles (Q3). Whiskers extend from Q1 to the smallest value within Q1 – 1.5* interquartile range (IQR) and from Q3 to the largest values within Q3 + 1.5* IQR. BF = Bayes Factor in favor of the alternative hypothesis.

1   We further investigated whether the sequences of microstates differed between

2   groups. To this end, transition probabilities from each microstate to all other microstates were

3   calculated for both the eyes-open and the eyes-closed conditions. Mean transition probabilities

4   for both groups and conditions as well as statistical results are presented in tables 4 and 5.

5   We found moderate evidence for a lower transition probability from microstates A and B to

6   microstate D in patients compared to controls in the eyes-open condition (Table 5; $3 < BF_{10} <$

7   10, FDR-corrected p-values = 0.103). Evidence for differences of all other transition

8   probabilities was either inconclusive or provided evidence for no group differences (see tables

9   4 and 5 for details).

10   In summary, the analysis of the temporal dynamics of microstates revealed a less

11   predominant role of microstate D in resting-state brain activity of chronic pain patients in both

12   eyes-open and eyes-closed conditions. No evidence for changes of the temporal

13   characteristics of microstates other than D was found.

14

15   **3.3. Relationships between temporal microstate characteristics and clinical**

16   **characteristics**

17   Having observed consistent evidence for changes of microstate D temporal characteristics in

18   patients with chronic pain, we explored whether microstate D temporal measures were

19   significantly related to clinical characteristics. To this end, we performed correlation analyses

20   between the temporal measures of microstate D and clinical parameters of the patients. We

21   specifically related microstate D characteristics to the current pain intensity, the SF-MPQ total

22   pain score as well as measures of depression (BDI) and medication (MQS). We only found

23   moderate evidence for an inverse relation between medication and the frequency of

24   occurrence of microstate D (Tables 6 and 7; eyes-closed: $BF_{10} = 4.16$, FDR-corrected p-value

25    $= 0.074$; eyes-open: $BF_{10} = 9.58$, FDR-corrected p-value = 0.050). Evidence for an association

26   between medication and the other microstate D measures was inconclusive (Tables 6 and 7;

27    $1/3 < BF_{10} < 3$). In addition, evidence for an association between the other clinical

1   characteristics and microstate D measures was either inconclusive or against an association

2   in both conditions (Tables 6 and 7).

3   Taken together, the results did not provide consistent evidence for relationships

4   between microstate D temporal measures and clinical characteristics.

4. Discussion

In the present study, we investigated the dynamics of brain function in patients suffering from chronic pain. To this end, we performed microstate analysis of resting-state EEG recordings in a large cohort of patients and age- and sex-matched healthy control participants. In both groups, resting-state brain activity could be described as sequences of 5 microstates labeled A to E. Analyses of the temporal characteristics of these microstates revealed a decreased presence of microstate D in patients as compared to healthy participants. These changes were consistently found in eyes-open and eyes-closed conditions. No evidence for differences in other microstates was found. Thus, the present findings describe microstate D-specific changes of the dynamics of brain function in resting-state EEG recordings of patients suffering from chronic pain.

Our analyses reveal shorter mean duration, lower time coverage, fewer occurrences and less explained variance of microstate D in patients compared to controls in both eyes-open and eyes-closed recordings. Thus, our findings robustly indicate a decreased presence of microstate D in resting-state EEG activity in patients suffering from chronic pain. These findings are in contrast to the only study which applied microstate analysis to resting-state EEG recordings of patients suffering from chronic pain so far [20]. That study found a lower occurrence and time coverage of microstate C in eyes-open resting state recordings of 43 patients. This difference between studies might at least in part be due to differences between patient groups. The previous study included 43 patients suffering from fibromyalgia whereas the present study included 101 patients suffering from different chronic pain conditions. Although the heterogeneous sample of the present study reflects clinical reality it might veil differences between chronic pain conditions. The two studies together might prompt further studies in larger groups of patients, ideally from different recording sites, to resolve this issue and to further clarify changes of microstates in chronic pain.

Our observations further complement recent fMRI studies, which have shown changes of the dynamics of brain function in chronic pain at ultra-low frequencies below 0.1 Hz (e.g. [3;

1   5; 10]). They extend this evidence by showing alterations of the dynamics of brain function at

2   frequencies higher than 1 Hz, in line with the *dynamic pain connectome* concept [28; 45].

3   Microstate analysis is an emerging tool for investigating the dynamics of brain activity.

4   Although the functional interpretation of microstates is not fully clear yet, microstate analysis

5   has been increasingly used to identify changes of brain dynamics in various neuropsychiatric

6   diseases [25; 34], which have furthered the understanding of the pathology of these disorders.

7   Beyond, alterations of microstates' characteristics might be useful as clinical biomarkers. For

8   instance, a recent study has identified the dynamics of microstates C and D as a promising

9   candidate endophenotype for schizophrenia [12]. However, our data did not provide evidence

10   for a correlation between alterations of microstate D and clinical characteristics. As the brain

11   processes discriminating chronic pain patients from healthy people differ from those encoding

12   momentary pain intensity [3; 32; 54; 58; 63], the observed changes might reflect the abnormal

13   disease state *per se* rather than its specific characteristics.

14   Microstate D has been related to attentional brain networks and functions (for reviews

15   see [34; 51]). In particular, microstate D has been associated with brain activity in fronto-

16   parietal regions [8; 11], the dorsal attentional control network [49] and focus-switching and

17   attentional reorientation [36]. Interestingly, deficits of cognitive function and particularly of

18   attentional switching have been extensively reported in patients suffering from chronic pain

19   [37]. A common hypothesis is that pain competes with other stimuli for limited cognitive

20   resources, thereby "demanding attention" and potentially impairing higher-order attentional

21   control mechanisms [17; 30; 56]. Thus, a decreased presence of microstate D might represent

22   a neurophysiological correlate of altered attentional functioning in chronic pain. However, as

23   we have not obtained direct measures of attentional functioning, we cannot directly test this

24   hypothesis in the present study. Future microstate studies on chronic pain might therefore

25   include tasks and/or questionnaires assessing attentional functions.

26   Several limitations of the current study need to be discussed. First, the specificity of the

27   decreased presence of microstate D for chronic pain is unclear. In particular, studies in patients

28   suffering from schizophrenia [12; 47] and major depressive disorder [38] also showed a

21

1   decreased presence of microstate D. However, investigating symptom- and disease-specificity

2   of these findings is challenging. Substantial progress in this endeavor requires large samples

3   of patients suffering from different neuropsychiatric symptoms and diseases, standardized

4   assessments and, ideally, sharing of data acquired at different sites. As a first step in that

5   direction, we share data and code of the present study in a standardized format with the

6   research community. Second, comparisons of microstate topographies showed slight but

7   statistically significant differences between patients and healthy controls. However,

8   considering these subtle differences together with the overwhelming similarity of microstate

9   topographies, the microstates of both groups likely capture the same underlying neural

10   networks. Third, the causal relationship between altered microstate dynamics and chronic pain

11   is unclear. First studies have shown that the dynamics of microstates can be changed by

12   neurofeedback [15] and non-invasive brain stimulation [53]. These approaches might thus be

13   useful to prove the causal link between changes in microstate dynamics and neuropsychiatric

14   disorders including chronic pain. Moreover, they highlight the potential utility of microstate

15   dynamics as targets for neurofeedback- and/or brain stimulation-based treatments of chronic

16   pain.

17   In conclusion, our findings provide evidence for altered dynamics of brain function in a

18   large cohort of chronic pain patients using EEG microstate analysis. We particularly observed

19   alterations of microstate D. As this microstate has been associated with attentional brain

20   networks and functions, changes of microstate D might relate to dysfunctional attentional

21   processes in chronic pain. These results add to the understanding of the pathophysiology of

22   chronic pain. Moreover, they might be useful for establishing a much sought-after EEG-based

23   biomarker of chronic pain.

24

Acknowledgments

References

[1] Allen M, Poggiali D, Whitaker K, Marshall TR, Kievit RA. Raincloud plots: a multi-platform tool for robust data visualization. Wellcome Open Res 2019;4:63.

[2] Baliki MN, Apkarian AV. Nociception, Pain, Negative Moods, and Behavior Selection. Neuron 2015;87(3):474-491.

[3] Baliki MN, Geha PY, Apkarian AV, Chialvo DR. Beyond feeling: chronic pain hurts the brain, disrupting the default-mode network dynamics. J Neurosci 2008;28(6):1398-1403.

[4] Beck AT, Steer RA, Brown G. Manual for the Beck Depression Inventory-II. San Antonio: TX: Psychological Corporation, 1996.

[5] Bosma RL, Kim JA, Cheng JC, Rogachov A, Hemington KS, Osborne NR, Oh J, Davis KD. Dynamic pain connectome functional connectivity and oscillations reflect multiple sclerosis pain. Pain 2018;159(11):2267-2276.

[6] Bréchet L, Brunet D, Birot G, Gruetter R, Michel CM, Jorge J. Capturing the spatiotemporal dynamics of self-generated, task-initiated thoughts with EEG and fMRI. NeuroImage 2019;194(February):82-92.

[7] Breivik H, Collett B, Ventafridda V, Cohen R, Gallacher D. Survey of chronic pain in Europe: prevalence, impact on daily life, and treatment. Eur J Pain 2006;10(4):287-333.

[8] Britz J, Van De Ville D, Michel CM. BOLD correlates of EEG topography reveal rapid resting-state network dynamics. NeuroImage 2010;52(4):1162-1170.

[9] Brunet D, Murray MM, Michel CM. Spatiotemporal analysis of multichannel EEG: CARTOOL. Computational intelligence and neuroscience 2011;2011:813870.

[10] Cheng JC, Rogachov A, Hemington KS, Kucyi A, Bosma RL, Lindquist MA, Inman RD, Davis KD. Multivariate machine learning distinguishes cross-network dynamic functional connectivity patterns in state and trait neuropathic pain. Pain 2018;159(9):1764-1776.

[11] Custo A, De Ville DV, Wells WM, Tomescu MI, Brunet D, Michel CM. Electroencephalographic Resting-State Networks: Source Localization of Microstates. Brain Connectivity 2017;7.

[12] da Cruz JR, Favrod O, Roinishvili M, Chkonia E, Brand A, Mohr C, Figueiredo P, Herzog MH. EEG microstates are a candidate endophenotype for schizophrenia. Nature communications 2020;11(1):3089.

[13] Davis JF. Manual of surface electromyography. WADC Technical Report (59-184). Montreal, Canada, 1959.

[14] Davis KD, Aghaeepour N, Ahn AH, Angst MS, Borsook D, Brenton A, Burczynski ME, Crean C, Edwards R, Gaudilliere B, Hergenroeder GW, Iadarola MJ, Iyengar S, Jiang Y, Kong JT, Mackey S, Saab CY, Sang CN, Scholz J, Segerdahl M, Tracey I, Veasley C, Wang J, Wager TD, Wasan AD, Pelleymounter MA. Discovery and validation of biomarkers to aid the development of safe and effective pain therapeutics: challenges and opportunities. Nature reviews Neurology 2020.

[15] Diaz Hernandez L, Rieger K, Baenninger A, Brandeis D, Koenig T. Towards Using Microstate-Neurofeedback for the Treatment of Psychotic Symptoms in Schizophrenia. A Feasibility Study in Healthy Participants. Brain Topogr 2016;29(2):308-321.

[16] Dillmann U, Nilges P, Saile H, Gerbershagen HU. [Assessing disability in chronic pain patients.]. Schmerz (Berlin, Germany) 1994;8(2):100-110.

[17] Eccleston C, Crombez G. Pain demands attention: a cognitive-affective model of the interruptive function of pain. Psychol Bull 1999;125:356-366.

[18] Freynhagen R, Baron R, Gockel U, Tolle TR. painDETECT: a new screening questionnaire to identify neuropathic components in patients with back pain. Current medical research and opinion 2006;22(10):1911-1920.

[19] Garrett DD, Samanez-Larkin GR, MacDonald SW, Lindenberger U, McIntosh AR, Grady CL. Moment-to-moment brain signal variability: a next frontier in human brain mapping? Neurosci Biobehav Rev 2013;37(4):610-624.

[20] Gonzalez-Villar AJ, Trinanes Y, Gomez-Perretta C, Carrillo-de-la-Pena MT. Patients with fibromyalgia show increased beta connectivity across distant networks and microstates alterations in resting-state electroencephalogram. Neuroimage 2020;223:117266.

1   [21] Harden RN, Weinland SR, Remble TA, Houle TT, Colio S, Steedman S, Kee WG.

2   Medication Quantification Scale Version III: update in medication classes and revised

3   detriment weights by survey of American Pain Society Physicians. J Pain

4   2005;6(6):364-371.

5   [22] JASP. JASP Team, 2020. (Version 0.13.1)[Computer software].

6   [23] Jung TP, Makeig S, Humphries C, Lee TW, McKeown MJ, Iragui V, Sejnowski TJ.

7   Removing electroencephalographic artifacts by blind source separation.

8   Psychophysiology 2000;37(2):163-178.

9   [24] Kennedy J, Roll JM, Schraudner T, Murphy S, McPherson S. Prevalence of persistent

10   pain in the U.S. adult population: new data from the 2010 national health interview

11   survey. J Pain 2014;15(10):979-984.

12 [25] Khanna A, Pascual-Leone A, Michel CM, Farzan F. Microstates in resting-state EEG:

13   current status and future directions. Neurosci Biobehav Rev 2015;49:105-113.

14 [26] Koenig T, Lehmann D, Merlo MC, Kochi K, Hell D, Koukkou M. A deviant EEG brain

15   microstate in acute, neuroleptic-naive schizophrenics at rest. Eur Arch Psychiatry Clin

16   Neurosci 1999;249(4):205-211.

17 [27] Koenig T, Prichep L, Lehmann D, Sosa PV, Braeker E, Kleinlogel H, Isenhart R, John ER.

18   Millisecond by Millisecond, Year by Year: Normative EEG Microstates and

19   Developmental Stages. NeuroImage 2002;16(1):41-48.

20 [28] Kucyi A, Davis KD. The dynamic pain connectome. Trends Neurosci 2015;38(2):86-95.

21 [29] Kuner R, Flor H. Structural plasticity and reorganisation in chronic pain. Nat Rev Neurosci

22   2017;18(2):113.

23 [30] Legrain V, Damme SV, Eccleston C, Davis KD, Seminowicz DA, Crombez G. A

24   neurocognitive model of attention to pain: behavioral and neuroimaging evidence. Pain

25   2009;144(3):230-232.

26 [31] Lehmann D, Faber PL, Galderisi S, Herrmann WM, Kinoshita T, Koukkou M, Mucci A,

27   Pascual-Marqui RD, Saito N, Wackermann J, Winterer G, Koenig T. EEG microstate

duration and syntax in acute, medication-naïve, first-episode schizophrenia: A multi-center study. Psychiatry Research - Neuroimaging 2005;138(2):141-156.

[32] May ES, Nickel MM, Ta Dinh S, Tiemann L, Heitmann H, Voth I, Tölle TR, Gross J, Ploner M. Prefrontal gamma oscillations reflect ongoing pain intensity in chronic back pain patients. Hum Brain Mapp 2019.

[33] Melzack R. The short-form McGill Pain Questionnaire. Pain 1987;30(2):191-197.

[34] Michel CM, Koenig T. EEG microstates as a tool for studying the temporal dynamics of whole-brain neuronal networks: A review. Neuroimage 2018;180(Pt B):577-593.

[35] Michel CM, Murray MM. Towards the utilization of EEG as a brain imaging tool. NeuroImage 2012;61(2):371-385.

[36] Milz P, Faber PL, Lehmann D, Koenig T, Kochi K, Pascual-Marqui RD. The functional significance of EEG microstates-Associations with modalities of thinking. Neuroimage 2016;125:643-656.

[37] Moriarty O, McGuire BE, Finn DP. The effect of pain on cognitive function: a review of clinical and preclinical research. Prog Neurobiol 2011;93(3):385-404.

[38] Murphy M, Whitton AE, Deccy S, Ironside ML, Rutherford A, Beltzer M, Sacchet M, Pizzagalli DA. Abnormalities in electroencephalographic microstates are state and trait markers of major depressive disorder. Neuropsychopharmacology : official publication of the American College of Neuropsychopharmacology 2020.

[39] Murray MM, Brunet D, Michel CM. Topographic ERP analyses: A step-by-step tutorial review. Brain Topography 2008;20(4):249-264.

[40] Nishida K, Morishima Y, Yoshimura M, Isotani T, Irisawa S, Jann K, Dierks T, Strik W, Kinoshita T, Koenig T. EEG microstates associated with salience and frontoparietal networks in frontotemporal dementia, schizophrenia and Alzheimer's disease. Clin Neurophysiol 2013;124(6):1106-1114.

[41] Oostenveld R, Fries P, Maris E, Schoffelen JM. FieldTrip: Open source software for advanced analysis of MEG, EEG, and invasive electrophysiological data. Computational intelligence and neuroscience 2011;2011:156869.

[42] Pascual-Marqui RD, Michel CM, Lehmann D. Segmentation of brain electrical activity into microstates: model estimation and validation. Ieee T Bio-Med Eng 1995;42(7):658-665.

[43] Pernet CR, Appelhoff S, Gorgolewski KJ, Flandin G, Phillips C, Delorme A, Oostenveld R. EEG-BIDS, an extension to the brain imaging data structure for electroencephalography. Sci Data 2019;6(1):103.

[44] Ploner M, May ES. Electroencephalography and magnetoencephalography in pain research - Current state and future perspectives. Pain 2018;159:206-211.

[45] Preti MG, Bolton TA, Van De Ville D. The dynamic functional connectome: State-of-the-art and perspectives. Neuroimage 2017;160:41-54.

[46] Rice AS, Smith BH, Blyth FM. Pain and the global burden of disease. Pain 2016;157(4):791-796.

[47] Rieger K, Diaz Hernandez L, Baenninger A, Koenig T. 15 Years of Microstate Research in Schizophrenia - Where Are We? A Meta-Analysis. Front Psychiatry 2016;7:22.

[48] Schumacher J, Peraza LR, Firbank M, Thomas AJ, Kaiser M, Gallagher P, O'Brien JT, Blamire AM, Taylor JP. Dysfunctional brain dynamics and their origin in Lewy body dementia. Brain 2019;142:1767-1782.

[49] Seitzman BA, Abell M, Bartley SC, Erickson MA, Bolbecker AR, Hetrick WP. Cognitive manipulation of brain electric microstates. Neuroimage 2017;146:533-543.

[50] Selim AJ, Rogers W, Fleishman JA, Qian SX, Fincke BG, Rothendler JA, Kazis LE. Updated U.S. population standard for the Veterans RAND 12-item Health Survey (VR-12). Qual Life Res 2009;18(1):43-52.

[51] Shaw SB, Dhindsa K, Reilly JP, Becker S. Capturing the Forest but Missing the Trees: Microstates Inadequate for Characterizing Shorter-Scale EEG Dynamics. Neural Comput 2019;31(11):2177-2211.

[52] Spielberger CD, Gorsuch RL, Lushene R, Vagg PR, Jacobs GA. Manual for the State-Trait Anxiety Inventory. Palo Alto: CA: Consulting Psychologists Press, 1983.

[53] Sverak T, Albrechtova L, Lamos M, Rektorova I, Ustohal L. Intensive repetitive transcranial magnetic stimulation changes EEG microstates in schizophrenia: A pilot study. Schizophr Res 2018;193:451-452.

[54] Ta Dinh S, Nickel MM, Tiemann L, May ES, Heitmann H, Hohn VD, Edenharter G, Utpadel-Fischler D, Tolle TR, Sauseng P, Gross J, Ploner M. Brain dysfunction in chronic pain patients assessed by resting-state electroencephalography. Pain 2019.

[55] Tomescu MI, Rihs TA, Becker R, Britz J, Custo A, Grouiller F, Schneider M, Debbané M, Eliez S, Michel CM. Deviant dynamics of EEG resting state pattern in 22q11.2 deletion syndrome adolescents: A vulnerability marker of schizophrenia? Schizophrenia Research 2014;157(1-3):175-181.

[56] Torta DM, Legrain V, Mouraux A, Valentini E. Attention to pain! A neurocognitive perspective on attentional modulation of pain in neuroimaging studies. Cortex 2017;89:120-134.

[57] Tracey I, Woolf CJ, Andrews NA. Composite Pain Biomarker Signatures for Objective Assessment and Effective Treatment. Neuron 2019;101(5):783-800.

[58] Tu Y, Fu Z, Mao C, Falahpour M, Gollub RL, Park J, Wilson G, Napadow V, Gerber J, Chan ST, Edwards RR, Kaptchuk TJ, Liu T, Calhoun V, Rosen B, Kong J. Distinct thalamocortical network dynamics are associated with the pathophysiology of chronic low back pain. Nature communications 2020;11(1):3948.

[59] Turk DC, Wilson HD, Cahana A. Treatment of chronic non-cancer pain. Lancet 2011;377(9784):2226-2235.

[60] Winkler I, Debener S, Muller KR, Tangermann M. On the influence of high-pass filtering on ICA-based artifact reduction in EEG-ERP. Conference proceedings : Annual International Conference of the IEEE Engineering in Medicine and Biology Society IEEE Engineering in Medicine and Biology Society Conference 2015;2015:4101-4105.

[61] Yekutieli D, Benjamini Y. Resampling-based false discovery rate controlling multiple test procedures for correlated test statistics. Journal of Statistical Planning and Inference 1999;82(1):171-196.

[62] Zanesco AP, King BG, Skwara AC, Saron CD. Within and between-person correlates of the temporal dynamics of resting EEG microstates. Neuroimage 2020;211:116631.

[63] Zhang B, Jung M, Tu Y, Gollub R, Lang C, Ortiz A, Park J, Wilson G, Gerber J, Mawla I, Chan ST, Wasan A, Edwards R, Lee J, Napadow V, Kaptchuk T, Rosen B, Kong J. Identifying brain regions associated with the neuropathology of chronic low back pain: a resting-state amplitude of low-frequency fluctuation study. Br J Anaesth 2019;123(2):e303-e311.

1   # Tables

2   **Table 1. Demographic data and questionnaire results**. BDI = Beck Depression Inventory;

3   STAI = State-Trait Anxiety Inventory; SF-MPQ = Short-form McGill Pain Questionnaire; VAS

4   = Visual Analogue Scale; Avg. pain intensity = average pain intensity in the past 4 weeks; PDI

5   = Pain Disability Index; PDQ = painDETECT; VR-12 PCS = Veteran's Rand 12 Physical

6   Component Summary; VR-12 MCS = Veteran's Rand 12 Mental Component Summary; MQS

7   = Medication Quantification Scale. Please note that data for avg. pain intensity in the past 4

8   weeks, pain duration and PDQ were only available for a subset of 81 patients. Data from PDI,

9   VR-12 PCS and VR-12 MCS were only available for a subset of 47 patients.

	Chronic pain patients (mean ± SD)	Healthy controls (mean ± SD)
Number	101	88
Gender (m/f)	32/69	28/60
Age (years)	58.2 ± 13.5	57.5 ± 14.3
BDI	15.8 ± 8.9	3.5 ± 4.5
STAI - State	39.5 ± 10.6	30.6 ± 6.1
STAI - Trait	44.0 ± 11.2	30.9 ± 7.1
SF-MPQ total pain score	27.1 ± 9.4	–
Current pain intensity (VAS)	5.2 ± 1.9	–
Avg. pain intensity in the past 4 weeks (VAS)	5.6 ± 1.6	–
Pain duration (months)	121.8 ± 114.4	–
PDQ	17.4 ± 6.5	–
PDI	27.4 ± 14.2	–
VR-12 PCS	31.8 ± 7.8	–
VR-12 MCS	46.4 ± 11.9	–
MQS	6.8 ± 8.1	–

10
11

1 **Table 2. Group comparisons of temporal microstate measures in the eyes-closed**

2 **condition.** Results of two-sided independent samples t-test (frequentist and Bayesian

3 approach). P-values are FDR-corrected. Color coded in red $p < 0.05$ and $BF_{10} > 3$, indicating

4 at least moderate evidence for the alternative hypothesis and in blue $BF_{10} < 1/3$, indicating at

5 least moderate evidence for the null hypothesis. Median effect sizes (δ) and their respective

6 95% credible interval (CI) are reported. Mean dur. = mean duration; Time cov. = time coverage;

7 Freq of occ. = frequency of occurrence; GEV = global explained variance; BF_{10} = Bayes Factor

8 in favor of the alternative hypothesis.

Microstate	Measure	t	p	BF_{10}	Median effect size (δ)	95% CI
A	Mean dur.	0.413	0.800	0.172	0.056	[-0.21, 0.334]
	Time cov.	0.608	0.679	0.189	0.083	[-0.194, 0.361]
	Freq of occ.	1.138	0.513	0.291	0.155	[-0.122, 0.435]
	GEV	0.212	0.832	0.162	0.029	[-0.248, 0.306]
B	Mean dur.	-1.831	0.228	0.754	-0.251	[-0.533, 0.028]
	Time cov.	-1.072	0.518	0.272	-0.146	[-0.426, 0.131]
	Freq of occ.	-0.298	0.806	0.166	-0.040	[-0.318, 0.236]
	GEV	-0.858	0.560	0.224	-0.117	[-0.396, 0.160]
C	Mean dur.	-0.654	0.679	0.194	-0.089	[-0.367, 0.188]
	Time cov.	-0.864	0.560	0.225	-0.118	[-0.397, 0.159]
	Freq of occ.	1.012	0.521	0.256	0.138	[-0.139, 0.417]
	GEV	-1.303	0.431	0.351	-0.178	[-0.458, 0.100]
D	Mean dur.	2.669	0.041	4.235	0.368	[0.085, 0.654]
	Time cov.	2.706	0.041	4.633	0.373	[0.090, 0.659]
	Freq of occ.	2.551	0.046	3.197	0.351	[0.069, 0.637]
	GEV	4.088	0.001	304.172	0.570	[0.280, 0.863]
E	Mean dur.	0.330	0.806	0.167	0.045	[-0.232, 0.322]
	Time cov.	-1.657	0.283	0.569	-0.226	[-0.508, 0.052]
	Freq of occ.	-1.348	0.431	0.371	-0.184	[-0.465, 0.094]
	GEV	-3.036	0.027	10.900	-0.419	[-0.707, -0.135]

9

1 **Table 3. Group comparisons of temporal microstate measures in the eyes-open**

2 **condition.** Results of two-sided independent samples t-test (frequentist and Bayesian

3 approach). P-values are FDR-corrected. Color coded in red $p < 0.05$ and $BF_{10} > 3$, indicating

4 at least moderate evidence for the alternative hypothesis and in blue $BF_{10} < 1/3$, indicating at

5 least moderate evidence for the null hypothesis. Median effect sizes (δ) and their respective

6 95% credible interval (CI) are reported. Mean dur. = mean duration; Time cov. = time coverage;

7 Freq of occ. = frequency of occurrence; GEV = global explained variance; BF_{10} = Bayes Factor

8 in favor of the alternative hypothesis.

Microstate	Measure	t	p	BF_{10}	Median effect size (δ)	95% CI
A	Mean dur.	-1.207	0.458	0.326	-0.171	[-0.465, 0.118]
	Time cov.	0.189	0.939	0.169	0.027	[-0.262, 0.317]
	Freq of occ.	0.943	0.534	0.251	0.134	[-0.156, 0.426]
	GEV	0.128	0.939	0.167	0.018	[-0.271, 0.308]
B	Mean dur.	-1.051	0.603	0.224	-0.114	[-0.406, 0.175]
	Time cov.	0.098	0.939	0.167	0.014	[-0.275, 0.304]
	Freq of occ.	1.317	0.421	0.370	0.187	[-0.103, 0.481]
	GEV	-0.726	0.624	0.212	-0.103	[-0.394, 0.186]
C	Mean dur.	-0.804	0.491	0.277	-0.149	[-0.442, 0.140]
	Time cov.	-1.417	0.395	0.420	-0.202	[-0.496, 0.089]
	Freq of occ.	-0.305	0.939	0.174	-0.043	[-0.333, 0.246]
	GEV	-1.418	0.395	0.421	-0.202	[-0.496, 0.089]
D	Mean dur.	2.828	0.026	6.402	0.407	[0.110, 0.708]
	Time cov.	2.938	0.026	8.501	0.423	[0.126, 0.725]
	Freq of occ.	2.942	0.026	8.595	0.424	[0.127, 0.726]
	GEV	2.922	0.026	8.159	0.421	[0.124, 0.723]
E	Mean dur.	-1.733	0.339	0.664	-0.247	[-0.543, 0.044]
	Time cov.	-1.145	0.461	0.305	-0.163	[-0.455, 0.127]
	Freq of occ.	-0.075	0.939	0.167	-0.011	[-0.300, 0.279]
	GEV	-1.486	0.395	0.461	-0.211	[-0.506, 0.079]

9

1 **Table 4. Group comparisons of transition probabilities between microstates in the eyes-**

2 **closed condition.** Results of two-sided independent samples t-test (frequentist and Bayesian

3 approach). P-values are FDR-corrected. Color coded in red $p < 0.05$ and $BF_{10} > 3$, indicating

4 at least moderate evidence for the alternative hypothesis and in blue $BF_{10} < 1/3$, indicating at

5 least moderate evidence for the null hypothesis. Median effect sizes (δ) and their respective

6 95% credible interval (CI) are reported. Mean trans. prob. = mean transition probability; CP =

7 chronic pain patients; HC = healthy controls; BF_{10} = Bayes Factor in favor of the alternative

8 hypothesis.

	Mean trans. prob. CP	Mean trans. prob. HC	t	p	BF_{10}	Median effect size (δ)	95% CI
From A to B	0.232	0.221	-0.595	0.920	0.188	-0.081	[-0.359, 0.196]
From A to C	0.388	0.388	0.005	1.000	0.159	0.001	[-0.276, 0.278]
From A to D	0.186	0.229	2.110	0.251	1.249	0.289	[0.009, 0.573]
From A to E	0.188	0.158	-1.808	0.299	0.724	-0.247	[-0.530, 0.032]
From B to A	0.223	0.224	0.073	1.000	0.160	0.010	[-0.267, 0.287]
From B to C	0.396	0.393	-0.111	1.000	0.160	-0.015	[-0.292, 0.262]
From B to D	0.190	0.235	2.310	0.251	1.873	0.317	[0.037, 0.602]
From B to E	0.187	0.145	-2.346	0.251	2.024	-0.322	[-0.607, -0.041]
From C to A	0.232	0.251	0.923	0.811	0.237	0.126	[-0.151, 0.405]
From C to B	0.257	0.231	-1.464	0.362	0.431	-0.200	[-0.481, 0.078]
From C to D	0.273	0.315	1.576	0.362	0.505	0.215	[-0.063, 0.497]
From C to E	0.235	0.201	-1.739	0.299	0.648	-0.238	[-0.520, 0.041]
From D to A	0.165	0.203	2.066	0.251	1.148	0.283	[0.003, 0.567]
From D to B	0.184	0.190	0.353	1.000	0.169	0.048	[-0.229, 0.326]
From D to C	0.398	0.411	0.483	0.983	0.177	0.066	[-0.211, 0.344]
From D to E	0.201	0.182	-0.848	0.828	0.222	-0.115	[-0.394, 0.161]
From E to A	0.193	0.207	0.726	0.902	0.203	0.099	[-0.178, 0.377]
From E to B	0.202	0.169	-1.873	0.299	0.810	-0.256	[-0.539,0.023]
From E to C	0.384	0.368	-0.648	0.920	0.193	-0.088	[-0.366, 0.189]
From E to D	0.216	0.253	1.489	0.362	0.446	0.203	[-0.075, 0.484]

9

1 **Table 5. Group comparisons of transition probabilities between microstates in the eyes-**

2 **open condition.** Results of two-sided independent samples t-test (frequentist and Bayesian

3 approach). P-values are FDR-corrected. Color coded in red $p < 0.05$ and $BF_{10} > 3$, indicating

4 at least moderate evidence for the alternative hypothesis and in blue $BF_{10} < 1/3$, indicating at

5 least moderate evidence for the null hypothesis. Median effect sizes (δ) and their respective

6 95% credible interval (CI) are reported. Mean trans. prob. = mean transition probability; CP =

7 chronic pain patients; HC = healthy controls; BF_{10} = Bayes Factor in favor of the alternative

8 hypothesis.

	Mean trans. prob. CP	Mean trans. prob. HC	t	p	BF_{10}	Median effect size (δ)	95% CI
From A to B	0.236	0.245	0.598	0.810	0.196	0.085	[-0.204, 0.376]
From A to C	0.388	0.341	-1.984	0.202	1.018	-0.283	[-0.580, 0.009]
From A to D	0.201	0.256	2.675	0.103	4.378	0.384	[0.089, 0.685]
From A to E	0.169	0.155	-0.756	0.810	0.217	-0.107	[-0.399, 0.182]
From B to A	0.244	0.243	-0.097	1.000	0.167	-0.014	[-0.303, 0.276]
From B to C	0.371	0.350	-0.816	0.810	0.226	-0.116	[-0.407, 0.173]
From B to D	0.194	0.248	2.865	0.103	7.042	0.412	[0.116, 0.714]
From B to E	0.186	0.156	-1.454	0.462	0.441	-0.207	[-0.501, 0.084]
From C to A	0.272	0.249	-1.234	0.609	0.336	-0.175	[-0.468, 0.115]
From C to B	0.264	0.260	-0.209	1.000	0.170	-0.030	[-0.319, 0.260]
From C to D	0.249	0.294	2.011	0.202	1.070	0.287	[-0.005, 0.584]
From C to E	0.209	0.194	-0.719	0.810	0.211	-0.102	[-0.393, 0.187]
From D to A	0.199	0.241	2.070	0.202	1.193	0.296	[0.003, 0.593]
From D to B	0.210	0.214	0.257	1.000	0.171	0.036	[-0.253, 0.326]
From D to C	0.371	0.355	-0.686	0.810	0.207	-0.097	[-0.388, 0.192]
From D to E	0.204	0.186	-0.804	0.810	0.224	-0.114	[-0.406, 0.175]
From E to A	0.205	0.196	-0.598	0.810	0.196	-0.085	[-0.376, 0.204]
From E to B	0.188	0.198	0.650	0.810	0.202	0.092	[-0.197, 0.383]
From E to C	0.386	0.342	-1.921	0.202	0.909	-0.274	[-0.571, 0.018]
From E to D	0.214	0.259	2.078	0.202	1.210	0.297	[0.004, 0.594]

9

1 **Table 6. Relationships between microstate D temporal measures and clinical**

2 **parameters in the eyes-closed condition.** Pearson's correlations (frequentist and Bayesian

3 approach) were performed for microstate D temporal measures, which had consistently shown

4 evidence for differences between patients and controls in previous analyses. P-values are

5 FDR-corrected. Color coded in red $p < 0.05$ and $BF_{10} > 3$, indicating at least moderate evidence

6 for the alternative hypothesis and in blue $BF_{10} < 1/3$, indicating at least moderate evidence for

7 the null hypothesis. ; BF_{10} = Bayes Factor in favor of the alternative hypothesis; 95% CI = 95%

8 credible interval; Mean dur. = mean duration; Time cov. = time coverage; Freq of occ. =

9 frequency of occurrence; GEV = global explained variance; SF-MPQ = short-form McGill pain

10 questionnaire; BDI = Beck's depression inventory; MQS = medication quantification scale.

		Current pain	SF-MPQ	BDI	MQS
Mean dur.	**Pearson's r**	0.123	0.071	0.061	-0.236
	p	0.504	0.580	0.580	0.074
	BF_{10}	0.260	0.160	0.150	1.974
	95% CI	[-0.075, 0.309]	[-0.126, 0.261]	[-0.136, 0.252]	[-0.408, -0.041]
Time cov.	**Pearson's r**	0.163	0.064	0.079	-0.238
	p	0.282	0.580	0.580	0.074
	BF_{10}	0.456	0.153	0.170	2.064
	95% CI	[-0.035, 0.345]	[-0.133, 0.255]	[-0.118, 0.269]	[-0.410, -0.043]
Freq. of occ.	**Pearson's r**	0.236	0.074	0.056	-0.265
	p	0.074	0.580	0.580	0.074
	BF_{10}	1.919	0.136	0.146	4.166
	95% CI	[0.039, 0.409]	[-0.124, 0.264]	[-0.141, 0.247]	[-0.434, -0.071]
GEV	**Pearson's r**	0.116	0.066	0.094	-0.189
	p	0.504	0.580	0.580	0.190
	BF_{10}	0.240	0.155	0.193	0.718
	95% CI	[-0.082, 0.302]	[-0.131, 0.257]	[-0.103, 0.283]	[-0.367, 0.008]

11

1   **Table 7. Relationships between microstate D temporal measures and clinical**

2   **parameters in the eyes-open condition.** Pearson's correlations (frequentist and Bayesian

3   approach) were performed for microstate D temporal measures, which had consistently shown

4   evidence for differences between patients and controls in previous analyses. P-values are

5   FDR-corrected. Color coded in red $p < 0.05$ and $BF_{10} > 3$, indicating at least moderate evidence

6   for the alternative hypothesis and in blue $BF_{10} < 1/3$, indicating at least moderate evidence for

7   the null hypothesis. ; BF_{10} = Bayes Factor in favor of the alternative hypothesis; 95% CI = 95%

8   credible interval; Mean dur. = mean duration; Time cov. = time coverage; Freq of occ. =

9   frequency of occurrence; GEV = global explained variance; SF-MPQ = short-form McGill pain

10   questionnaire; BDI = Beck's depression inventory; MQS = medication quantification scale.

		Current pain	SF-MPQ	BDI	MQS
Mean dur.	**Pearson's r**	0.191	0.108	0.177	-0.164
	p	0.279	0.434	0.279	0.279
	BF_{10}	0.648	0.218	0.514	0.427
	95% CI	[-0.018, 0.379]	[-0.101, 0.304]	[-0.032, 0.366]	[-0.354, 0.044]
Time cov.	**Pearson's r**	0.129	0.023	0.124	-0.262
	p	0.394	0.881	0.394	0.099
	BF_{10}	0.272	0.136	0.256	2.861
	95% CI	[-0.080, 0.324]	[-0.183, 0.227]	[-0.085, 0.319]	[-0.440, -0.057]
Freq. of occ.	**Pearson's r**	0.168	-0.016	0.048	-0.308
	p	0.279	0.881	0.804	0.051
	BF_{10}	0.449	0.134	0.146	9.589
	95% CI	[-0.041, 0.358]	[-0.220, 0.190]	[-0.159, 0.250]	[-0.478, -0.105]
GEV	**Pearson's r**	0.105	0.017	0.154	-0.220
	p	0.434	0.881	0.301	0.200
	BF_{10}	0.213	0.134	0.366	1.106
	95% CI	[-0.104, 0.302]	[-0.189, 0.221]	[-0.056, 0.345]	[-0.402, -0.012]

11